La mer 38 : 189–198, 2000
Société franco-japonaise d'océanographie, Tokyo

Circulation patterns of the Japan Sea

Vladimir PONOMAREV* and Olga TRUSENKOVA*

Abstract : The current system and characteristic circulation patterns in the Japan Sea are simulated using the MHI numerical layered model (Marine Hydrophysical Institute, Sebastopol, Ukraine) which can treat features of the large/synoptic scale dynamic processes over the irregular bottom topography. The model is forced mainly by heat and buoyancy fluxes through the straits and sea surface. Numerical experiment is performed from Levitus climatology temperature initial conditions. In model spin-up from the smooth initial density distribution, the system of jet currents and fronts is formed due to layer outcropping. Principal circulation features such as the Liman Current, East Korean Warm Current, Offshore and Nearshore Tsushima Current Branches, known from observation and simulations performed earlier by many authors are simulated. The numerical result obtained on 1/16° grid is characterized by current branching in the northwest sea area and multiple structure of the Subarctic Front. The synoptic scale features in the main pycnocline such as meandering, cyclonic/anticyclonic eddies and streamers are simulated.

Key words : *Japan Sea, sea circulation, numerical simulation, synoptic dynamic structures*

1. Introduction

The Japan Sea is a weakly stratified deep marginal sea connected to the Pacific Ocean, East China Sea and Sea of Okhotsk by shallow straits. The transformed subtropical water is directly transported through the Japan Sea to the oceanic transitional area between the subtropic and subarctic gyres and to the Sea of Okhotsk by inflow into the Tsushima (Korean) Strait and outflow to the Tsugaru and Laperus (Soya) Straits.

The Japan Sea is characterized by shallow pycnocline (down to 250–300 m in the southern sea and only seasonal one down to 50 m in the northern sea) and an almost homogeneous cold deep water mass known as the Japan Sea Proper Water underneath. The Subarctic (Polar) Front at about 39°–40°N separates the southern and northern areas.

More than 100 years of oceanographic observations in the Japan Sea established the principal features of the sea circulation. There is a cyclonic gyre in the northern Japan Sea formed by the East Korean Warm Current (EKWC) flowing north- and northeastward and by the North Korean Cold Currents flowing south- and southwestward Liman and North Korean Cold Currents. The circulation is mostly anticyclonic in the southern Japan Sea, characterized by the three current branches entering the sea through the Tsushima Strait. They are baroclinic EKWC, baroclinic unstable Offshore Tsushima Branch flowing mostly along 1000 m isobath with countercurrent in lower layer and barotropic Nearshore Branch along 200 m isobath (YOON, 1991).

In the recent decades, satellite and high-accuracy CTD and ADCP observations have emphasized the important role of synoptic scale processes in the Japan Sea. Meandering and branching of the main currents, quasi-stationary and moving eddies have been revealed in the southwestern and southeastern sea areas, over the Yamato Rise, and in Northwestern Japan Sea (ICHIYE and TAKANO, 1988; OSTROVSKII and HIROSE, 1994; DANCHENKOV *et al.*, 1997).

Recent numerous numerical simulations based on different models reproduced most of the large scale flow patterns in the Japan Sea mentioned above. Some mechanisms were

* Pacific Oceanological Institute, 43 Baltiyskaya, Vladivostok, 690041, Russia
e-mails: archer@stl.ru, ponom@t.kanazawa-t.ac.jp, trolia@ocean.poi.dvo.ru

revealed such as wind stress curl or/and buoyancy forcing, and topographical control (YOON, 1991; SEUNG and KIM, 1993; HOLLOWAY *et al.*, 1995; HOGAN and HURLBURT, 1997; MOOERS and KANG, 1997). The frequently arising problems, such as overshooting of EKWC, absence of one of the Tsushima Current branches, and modeling of deep water circulation were also discussed. Features of the synoptic scale dynamics were also simulated by high-resolution models (RO, 1999). The crucial factor is parameterization of horizontal and vertical friction/turbulent diffusion which is accounted for different manner among various models, such as reduced gravity models, Holloway's model, Princeton University model (POM), and layered models.

The goal of this study is to demonstrate the circulation patterns in the Japan Sea simulated by a layered model which allows substantial isopycnal turbulent momentum/heat/salt exchange while diapycnal turbulent fluxes between inner layers are set up low or negligible. Vertical change of baroclinic component of horizontal velocity may be expected to be more realistic.

2. MHI hydrodynamic model and setup of the numerical experiment

The MHI numerical layered model of sea circulation is developed by MIKHAILOVA and SHAPIRO, (1992), SHAPIRO (1998) in the Marine Hydrophysical Institute (MHI), Sebastopol, Ukraine. It is based on the primitive equations under the hydrostatic and Boussinesq approaches. The MHI model consists of a turbulent upper mixed layer (UML) and any number of inner layers with temperature and salinity integrated vertically within layers but being functions of time and horizontal coordinates. UML approximation is, mostly, similar to that employed in BLECK *et al.* (1989). Parameterizations of buoyancy, heat and salt fluxes on the sea surface, bottom of UML and other layer interfaces have been comprehensively described in MIHAYLOVA and SHAPIRO, (1992) and SHAPIRO (1998). Both entrainment and detrainment (subduction) regimes are allowed for UML. Note, that employing non-homogeneous inner layers makes easier subduction approximation in the MHI model compared to most isopycnal models, such as BLECK *et al.* (1989). Buoyancy variations in inner layers are limited by the so-called "base" stratification:

$$b^{\sigma}{}_{k} \leq b_{k} < b^{\sigma}{}_{k-1} \qquad \text{for } k \geq 2, \tag{1}$$

where $b^{\sigma}{}_{k}$ is the kth layer base buoyancy ($b^{\sigma}{}_{k} > b^{\sigma}{}_{k+1}$) and b_{k} is the kth layer buoyancy, and $b^{\sigma}{}_{n} = 0$, $b^{\sigma}{}_{0} = \infty$. If buoyancy of an inner layer gets out of its "base" limits, the layer outcrops, acquiring zero thickness and becoming dynamically inactive and transparent for mass, heat and salt fluxes.

As for boundary conditions, normal components of velocity, heat and salt fluxes are equal to zero at the sea bottom. Bottom friction and friction between layers are set up as square functions of horizontal velocity shear. At lateral walls, no slip condition is imposed, and no heat or salt flux is allowed. In inflow/outflow ports, volume transport, temperature, salinity, and inflow-outflow layers thickness are given in an annual cycle. At the sea surface, kinematic boundary condition for vertical velocity, wind stress, and equations of heat and salt balance are given (SHAPIRO, 1998). Annual cycle of air temperature, incoming short-wave solar radiation, wind velocity, cloudiness, and precipitation is taken into account to calculate buoyancy flux through the sea surface. The model can be forced by climatic or synoptic winds. The model equations, conditions at layer interfaces, finite difference approximation and methods of the numerical solution are described in MIKHAILOVA and SHAPIRO, (1992) and SHAPIRO (1998).

Bottom topography used in the model run is introduced by scaling initial sea depth:

$$Z_{n}'(x,y) = Z_{m} + \alpha \cdot [Z_{n}(x,y) - Z_{m}], \tag{2}$$

where $Z_{n}(x,y)$, $Z_{n}'(x,y)$, are initial and scaled sea depth and Z_{m} is mean sea depth. Scaling factor α is equal to 0.7, scaled sea depth is further smoothed by 9-point filter.

We performed the initial spin-up simulation with horizontal resolution of 1/16° (5-7 km) to obtain temperature, salinity, layer interfaces, and horizontal velocity fields adapted to the summer external conditions including weak climatic wind and bottom topography. Vertical

resolution of 7 layers including UML and 6 inner layers is chosen so that the 2nd layer corresponds to a layer of subtropical water, 3rd – 5th layers represent the main pycnocline, and 6th –7th layers describe deep waters of the Japan Sea (Japan Sea Proper Water).

Initial condition of summer Levitus climatology is chosen for temperature in layers 1 – 6 referenced to the layer middle depth, while a constant value of 0.06°C is accepted for the lowest 7th layer. Horizontally homogeneous initial salinity is set up as 33.5, 33.7, 34.00, 34.02, 34.05, 34.06, and 34.077 psu. Flat initial interfaces between layers are defined at 5, 50, 100, 150, 250, and 500m depth. As density gradient is supported mostly by temperature gradient in the Japan Sea, initial condition as described is chosen intentionally with the purpose to study the simulated field adaptation, especially of salinity and layer interfaces started from homogeneous state. Base buoyancy is chosen as 10 (∞), 2.1, 1.3, 1, 0.83, 0.72, and 0.

The subtropical water enters into the Japan Sea through the Tsushima Strait (of 100 m depth, layers 1–3), with temperature of 26/20 ℃, salinity of 34.4/34.6 psu and total volume transport of 1.5 Sv. The entered water volume flows out from the Japan Sea through the Tsugaru and Laperus (Soya) Straits (of 100 and 50 m depth) divided between them in ratio of 2:1. The simulation is performed under forcing of weak summer climatic wind. Starting date is the 1st of June. The following coefficients are used in the simulation: 2.5×10^{8} m^4/s for bi-harmonic isopycnal viscosity, 25 m^2/s for isopycnal harmonic viscosity and diffusion, and 5×10^{-8} m^2/s for diapycnal mixing. Note, that bi-harmonic viscosity is applied, while harmonic viscosity is switched on only when needed to suppress checkerboard noise.

3. Simulation of the circulation patterns in the Japan Sea

Spin-up simulation started from Levitus climatology generally describes main current systems of the northern and southern Japan Sea as early as in 40 days of integration (Figs. 1–2). Temperature, horizontal velocity, initially homogeneous salinity and layer interfaces become adapted to each other and to the bottom topography, total kinetic energy reaches quasi-stationary state in 10–12 days. Sea surface height developed in 40 days of integration shows cyclonic gyre in the northern Japan Sea and anticyclonic circulation in the southern sea (not shown). The pattern is similar to that simulated by other authors, such as YOON, (1991), SEUNG and KIM, (1993), HOLLOWAY *et al.* (1995), MOOERS and KANG, (1997), HOGAN and HURLBURT (1997), and RO (1997). Sea surface height difference of about 20 cm between northern and southern sea areas is similar to that derived from altimetry data assimilation (HIROSE and OSTROVSKII, 1994).

In the Northern Japan Sea, Primorye (Liman) Current is obtained as an irregular stream intensified along the Primorye coast to the south of 44°30′ N with general cyclonic circulation in the Peter the Great Bay near Vladivostok. It reaches southward as far as 40° N where it becomes the coastal countercurrent in relation to the northeastern branch of the East Korean Warm Current (EKWC) flowing along the continental slope and turning eastward from the slope (Fig. 1).

The Shrenk (Liman) Current is obtained in the Northern Tatar Strait from 52° to 49° N with general cyclonic circulation in the Strait (Figs. 1–2). There exists northeastward stream from 45° to 49° N along the Siberian coast from sea surface down to 500 m (1st – 5th layers). That is coincident with the observation in summer described by YURASOV and YARICHIN (1991). They explained the northward and northeastward surface currents along the Northern Primorye coast to be caused by the summer monsoon. On the contrary, Primorye Current along the most areas of the northwestern sea coast is intensified under forcing of winter synoptic wind conditioned by the winter monsoon as shown in PONOMAREV and YURASOV (1994), and PONOMAREV and TRUSENKOVA (2000a).

The northern EKWC branch carries transformed subtropical water to the north to the Laperus (Soya) and Tatar Straits and is usually associated with the Northern Front (Fig. 1) of the interfrontal zone between 38°–40°30′ N. The 2nd layer outcrops in the north of this jet, where UML comes into contact with the 3rd layer and the water from the 2nd layer gets

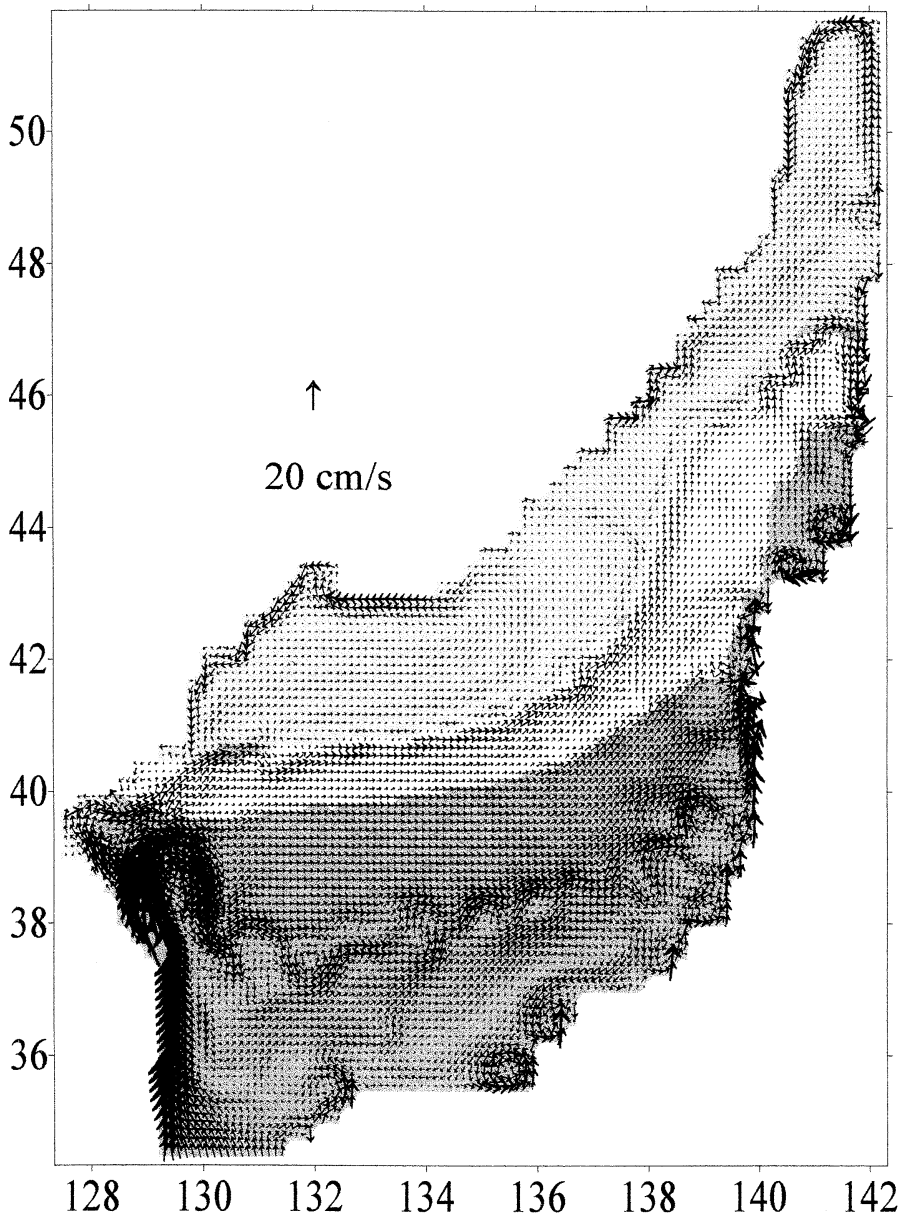

Fig. 1. Horizontal velocity in the UML in every 4th grid point. The northern area where the 2nd layer outcrops, is filled with smoke-grey; the interfrontal zone, where the 3rd layer outcrops but the 2nd layer does not, is filled with white, and the southern area, where the layers do not outcrop, is painted with charcoal grey.

involved into the 3rd layer. The 3rd layer outcrops in the interfrontal zone where the 2nd layer contacts the 4th layer with water from the 3rd layer entering the 2nd layer (Figs. 1 and 2). Two main, northern and southern fronts and a subsurface intermediate front between them are clearly seen in slopes of interface depth between 2nd and 3rd layers and 3rd and 4th layers (Fig. 3a, b). The northern front manifests itself in UML velocity (Fig. 1),

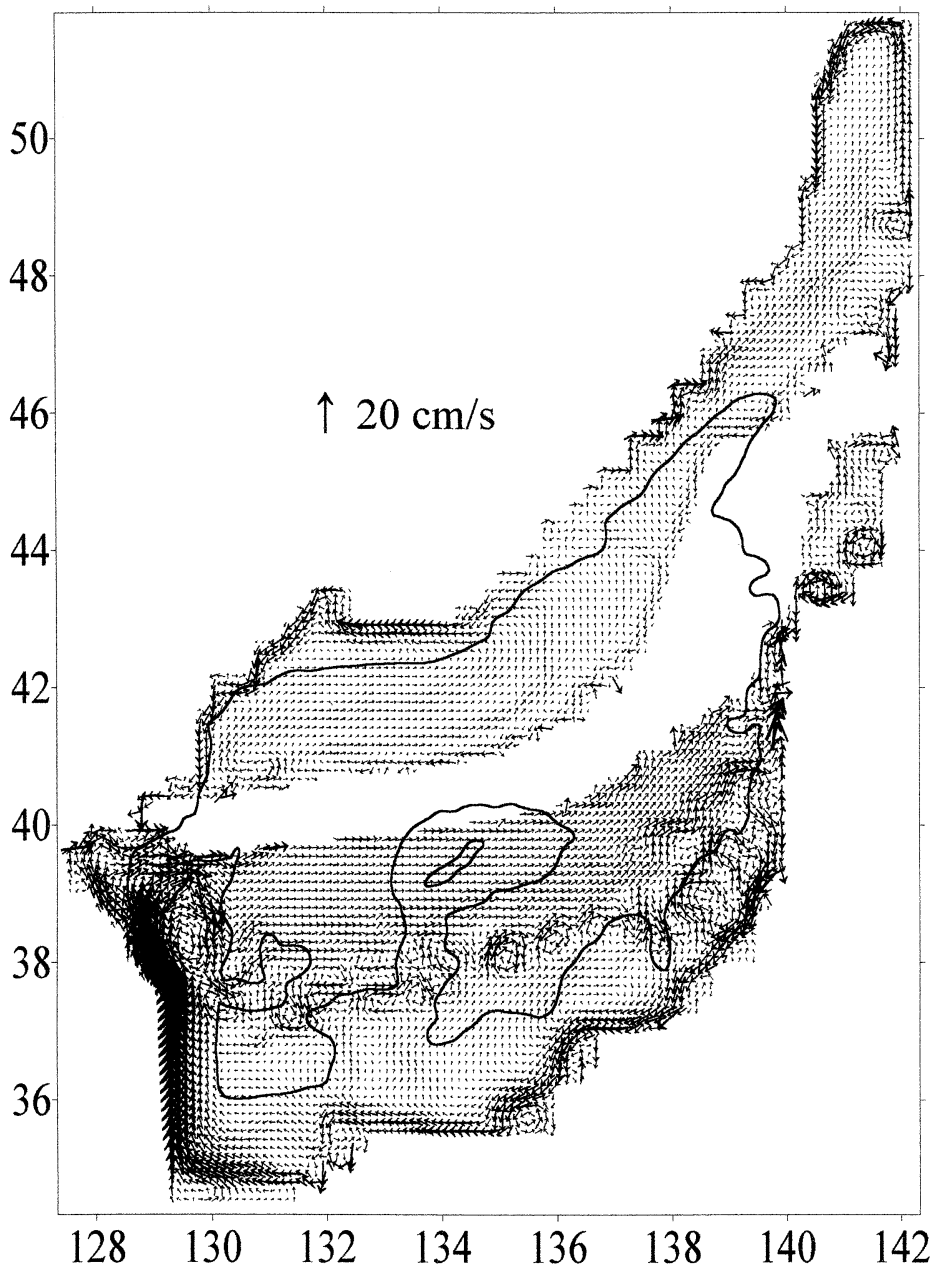

Fig. 2. Horizontal velocity in the 3rd layer. Velocity vectors are shown in every 4th grid location. The layer outcrops in the interfrontal zone where there is no arrows. 1500 m contour of bottom topography is shown.

temperature and in less extent salinity (not shown). The southern front can be seen in UML, 2nd and 3rd layers temperature, salinity, horizontal velocity and depths of interfaces between layers (Figs. 1–3).

Figure. 2 shows countercurrents in the main pycnocline of the interfrontal zone, with an eastward and northeastward current along the southern edge of 3rd layer outcropping area and a westward and southwestward current

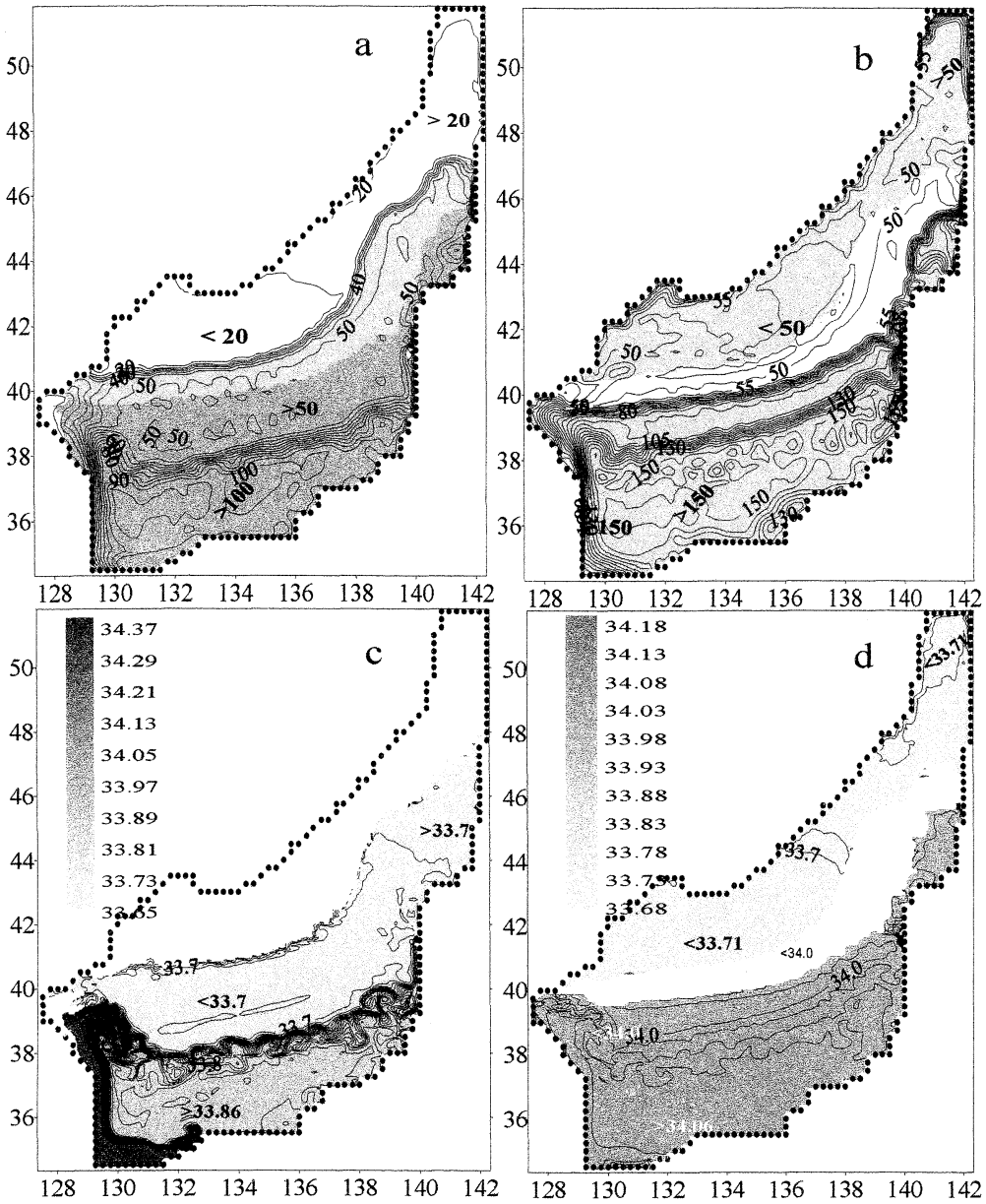

Fig. 3. Topography (contours every 5 m) of lower interfaces (a, b) and salinity (c, d) in the 2nd (a, c) and 3rd (b, d) layers (salinity contours every 0.01 psu in (c) and 0.005 psu in (d)). In (a, c) the northern area where the 2nd layer outcrops, and in (b, d) the interfrontal zone where 3rd layer outcrops are white. In (a, d) the southern area where both the 2nd and 3rd layers do not outcrop is filled with charcoal grey.

along its northern edge. There is a countercurrent at the northern/northwestern edge of the Northern Front in UML (Fig. 1). Countercurrents and convergence/divergence areas were earlier reported in the interfrontal zone, based on observation data (YURASOV and YARICHIN, 1991).

The subsurface intermediate front is well

pronounced in the 3rd layer temperature (not shown) and salinity (Fig. 3d). The 3rd layer temperature (8–9 ℃) is higher in the north of the outcropping area than that to the south (7–8℃). This should be attributed to the fact that in this area the 3rd layer carries warmer water mass from the initial 2nd layer.

Initial salinity is taken constant in layers, unlike Levitus climatological initial temperature. Nevertheless, salinity field formed in the upper layers during 40-days spin-up reveals lower values in the north and, especially, in the northwest Japan Sea. The intermediate front separates the subtropical high salinity water in the south (34 psu and more) from the low salinity waters in the north (33.71 psu and less; Fig. 3c). Moreover, starting from vertically increasing initial salinity, a belt of lower salinity is formed along this front in the southern area just in 40 days of integration, although the difference is very small (33.99 psu versus 34.00 psu; Fig. 3c). It is a result of anti-entrainment (subduction) from the upper layers, i.e., the temporal variable process which would form salinity minimum layer in the southern sea. Intermediate layer of lower salinity is a feature of the water structure in the Southern Japan Sea, well known from observations (YURASOV and YARICHIN, 1991).

The northern and southern fronts were earlier revealed from oceanographic observations (Zuenko, 1999). The simulation performed in this study shows that the Subarctic Frontal Zone in the Japan Sea should be associated with the multiple front system.

As for the southern current system, the three known branches (YOON, 1991) are obtained in this simulation, namely, EKWC (western branch), central (the Offshore Branch) and eastern coastal (Nearshore Branch) Tsushima Current branches.

EKWC flows as an intensified western boundary current along the Korean continental slope as far north as 39°–40° N where it bifurcates with separating off the slope. Similar double branch structure of EKWC was found based on trajectories of drift bottles (MIITA and KAWATATE, 1986). It is known from observations (YURASOV and YARICHIN, 1991) that EKWC separates from the coast at 37° – 38° N, so our simulation shows an "overshooting" of EKWC (Figs. 1 and 2). In some studies overshooting is explained by insufficient horizontal grid resolution and high coefficients of isopycnal mixing. For example, overshooting occurs on 1/8° – 1/16° grids but disappears on 1/32° grid in HOGAN and HURLBURT, (1997). However, it seems in our simulation that it is due to insufficient time of integration from the initial Levitus temperature fields interpolated from the coarse 1° grid to the fine 1/16° grid. When started from horizontally homogeneous initial conditions, we obtained EKWC separating from the coast at 37° N even on 1/4° grid (PONOMAREV and TRUSENKOVA, 2000 b). Cyclonic gyre in the Northwest Japan Basin area adjacent to the Primorye and North Korea is clearly seen in Figs. 1 and 2.

While separating from the slope, the southern EKWC branch forms a strong anticyclonic meander over the top of the Korean Plateau centered at 38° 20′ N, 129° 30′ E. The similar meander and eddy was reported in KATOH (1994) based on ADCP and hydrographic data although it was positioned to be at about 1° southward. In the east of the meander, the EKWC joins with the Offshore Branch of the Tsushima Current.

The Tsushima Offshore Branch associated with the southern front of the Subarctic Frontal Zone is the current meandering over the eastern slope of the Yamato Basin pronounced in UML, 2nd and 3rd layers (Figs.1, 2 and 4). It is characterized by a chain of baroclinic eddies generated in pycnocline due to baroclinic instability. According to the vertical velocity profile at the edge of an anticyclonic eddy (38° 6′ N, 134° 50′ E; location shown as a black dot in Fig. 4b) in Fig. 5a, velocity in UML, 2 nd, 3rd, 4th, 6th and 7th layers has values of 13.4, 15.2, 10.4, 3.4, 0.7 and 0.5 cm/s, respectively (the 5th layer outcrops to the 4th layer in this grid location). Velocity is more than 10 cm/s down to 145m (interface between 3rd and 4th layers), with maximum (15.2 cm/s; Fig. 5 a) in the 2nd layer. Vertical velocity profile averaged over the sea also has its maximum (34 cm/s; Fig. 5b) in the 2nd layer corresponding to depth of highest vertical gradient of buoyancy. Subsurface velocity maximum can be associated with

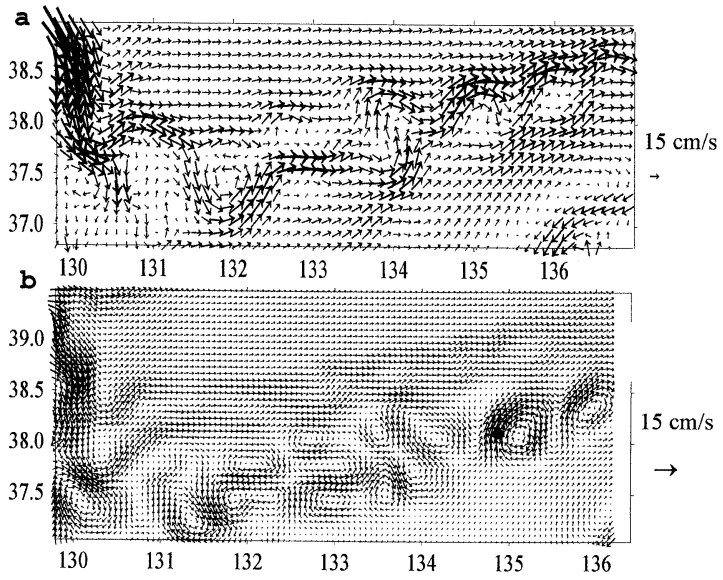

Fig. 4. A chain of baroclinic eddies in the Offshore Tsushima Branch as seen in horizontal velocity in the 2nd (a) and 3rd (b) layers. A black dot denotes location of the velocity vertical profile from Fig. 5a.

synoptic scale dynamics. However, in this area there is no immediate trace of pycnocline eddies in the 6th and 7th thick layers of deep waters, where another kind of synoptic scale circulation develops, mostly controlled by bottom topography.

Figure 4 shows some features of synoptic scale dynamics in the area of the Offshore Tsushima Current, namely branches, meanders, streamers, mushroom-like structures, cyclonic and anticyclonic eddies packed in pairs, quadruples and chains. Between 130° E and 134° E the synoptic scale current bifurcates in the 2nd layer (Fig. 4a) and a complicated eddy structure in the pycnocline in the 3rd layer (Fig. 4b) is formed. In the east of 134°30′ E, with periodic in space meanders and jet streams (streamers) in UML and 2nd layer, there are three anticy-clonic eddies in the 3rd layer with a diameter of 60–70 km.

Warm eddies with such scale were observed also in the southern Japan Sea (ICHIYE and TAKANO, 1988; DANCHENKOV *et al.*, 1997 and others). Different flow patterns in UML, 2nd and 3rd layers should be attributed mostly to low coefficient of diapycnal mixing.

The meandering Offshore Branch can be clearly traced at the depth of interface between the 2nd–3rd and 3rd–4th layers (Fig. 3a, b). Both temperature and salinity in UML, 2nd, and 3rd layers reveal meandering and spiral patterns along the Offshore Branch path an the 37°–38° N band (Fig. 3c, d).

The Nearshore Tsushima Branch is not very well pronounced in our results. It occupies 4 grid points adjacent to the Japanese coast in UML (Fig. 1) and also in the 2nd, upper inner layer, with its lower interface at the depth of about 100 m. Poor development of the coastal branch in the initial spin-up experiment should be attributed to the same reasons as overshooting of EKWC, namely to short time of integration and coarse resolution of initial temperature field.

4. Conclusions

The MHI circulation model successfully simulates the general circulation of the Japan Sea in initial 40-day spin-up from the climatological (Levitus) density distribution with 1/16° horizontal resolution under forcing of weak summer climatic wind. It coincides with numerous oceanographic observations in the sea and many previous simulations based

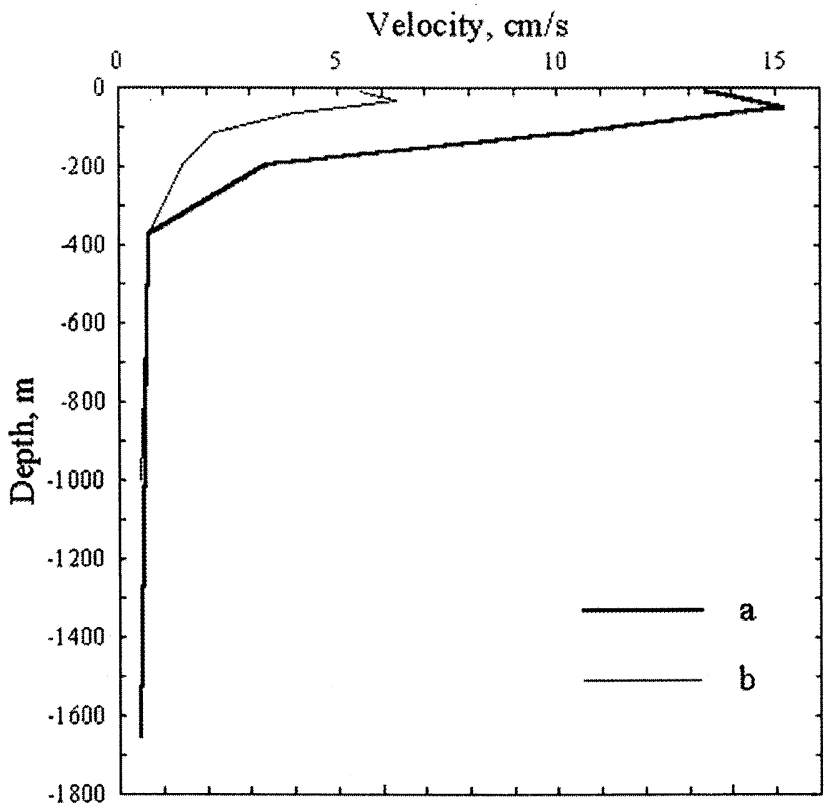

Fig. 5. Vertical profiles of horizontal velocity at the (38°6′N, 134°50′E) grid location (a) and averaged over the sea (b).

on different models. Two faults of our spin-up simulation are overshooting of EKWC and poor development of the Nearshore Tsushima Current Branch. However, these deficiencies are avoided in 40-year model run from horizontally homogeneous initial condition despite the coarse resolution of 1/4° grid (PONOMAREV and TRUSENKOVA, 2000b).

Subduction algorithm provided by coupling of non-homogeneous both UML and inner layers allows formation of a belt of lower salinity and, later, salinity minimum layer in the main pycnocline, starting from vertically increasing initial salinity distribution.

By allowing layer outcropping, the MHI model realistically reproduces frontal interfaces.

The numerical result is characterized by the branching of current in the northwest sea and multiple structure of the Subarctic Front. The synoptic scale features are simulated in the main pycnocline such as meandering, cyclonic /anticyclonic eddies and streamers. These synoptic scale patterns are due to baroclinic instability in the area of the Southern Subarctic Front characterized by well pronounced main pycnocline. Application of bi-harmonic rather than harmonic isopycnal viscosity as well as of low coefficient of diapycnal mixing and non-linear interface friction favors different flow patterns in UML, 2nd and 3rd layers.

References

BLECK, R., H. P. HANSON, D. HU, and E. B. KRAUS (1989): Mixed layer-thermocline interaction in a three dimensional isopicnic coordinate model. J. Phys. Oceanogr., **19**, 10: 1417-1439.

DANCHENKOV, M. A., V. B. LOBANOV, and A. A. NIKITIN (1997): Mesoscale eddies in the Japan Sea. Their role in circulation and heat transport. Proc. of the CREAMS'97 Int. Symp., Fukuoka, Japan, 28-30 Jan. 1997, 81-84.

HOGAN, P. J., and H. E. HURLBURT (1997): Sea of Japan

circulation dynamics via the NRL layered ocean model. Proc. of the CREAMS'97 Int. Symp., Fukuoka, Japan, 28–30 Jan. 1997, 109–112.

HOLLOWAY, G., T. SOU, and M. EBY (1995): Dynamics of circulation of the Japan Sea. Journal of Marine Research, **53**, 539–569.

ICHIYE, T., and K. TAKANO (1988): Physical structure of eddies in the Southwestern East Sea. La mer, **26**, 69–75.

KATOH, O. (1994): Tsushima Current in the south-western Japan Sea, J. Phys. Oceanogr., **50**, 317–338.
MIITA, T. And K. KAWATATE (1986): Trajectories of drift bottles released in the Tsushima Strait. Progress of Oceanography, **17**, 255–263.

MIKHAYLOVA, E. N., and N. B., SHAPIRO, (1992): Quasi-isopycnal multilayer model of large-scale ocean circulation. Morskoy Gidrophysicheskiy Journal Sebastopol, USSR, **4**, 3–13, (in Russian).

MIITA, T., and K. KAWATATE (1986): Trajectories of drift bottles released in the Tsushima Strait. Progress of Oceanography, **17**, 255–263.

MOOERS, C. N. K., and H. S. KANG (1997): On the 26 sigma level POM model for Japan (East) Sea circulation. Proc. of the CREAMS'97 Int. Symp., Fukuoka, Japan, 28–30 Jan. 1997, 15–17.

OSTROVSKII, A., and Y. HIROSE (1994): The Japan Sea circulation as seen in satellite infrared imagery in autumn 1993. Proc. CREAMS 94, 24–26 Jan. 1994, Fukuoka, Japan, 129–133.

PONOMAREV, V. I., and O. O. TRUSENKOVA (2000a): The dynamic response to the wind and buoyancy forcing in the Sea of Japan. Proc. of Int. Conf. on coastal ocean., Moscow, Russia, Sep. 1998, 99–108.

PONOMAREV, V. I., and O. O. TRUSENKOVA (2000b): Simulation of the Japan Sea circulation in summer 1999 using the MHI layered model. Proceedings of CREAMS–2000 Fourth Int. Symp., May 15–16, 2000, Vladivostok, Russia (in press).

PONOMAREV, V. I., and G. I. YURASOV (1994): The Tartar (Mamiya) Strait Currents. Journal of the Korean Society of Coastal and Ocean Engineers, **6**, 335–339.

RO, Y.J. (1999): Numerical experiments of the meso scale eddy activities in the East (Japan) Sea. Proc. of the CREAMS'99 Int. Symp., Fukuoka: 116–119.

SEUNG, Y. H., and K. KIM (1993): A numerical modeling of the East Sea circulation. Journal of the Oceanological Society of Korea, **28**, 292–304.

SHAPIRO, N. B. (1998): Formation of the Black Sea general circulation considering stochastic wind stress. Morskoy Gidrophysicheskiy Journal, Sebastopol, Ukraine, **4**, 12–24 (in Russian).

YOON J.-H. (1991): The branching of the Tsushima Current/ Rep. Res. Inst. Appl. Mech. Kyushyu Univ., **38**, 1–21.

YURASOV G. I., and V. G. YARICHIN (1991): Currents of the Japan Sea. Vladivostok, 173 pp (in Russian).

ZUENKO, Yu. (1999): Two decades of Polar Front large-scale meandering in the North-western Japan Sea. Proc. of the CREAMS'99 Int. Symp., Fukuoka: 68–71.

Recived on February 10, 2000
Accepted on November 2, 2000